Japanese Journal of
Oncology and Clinical Research

JScholar
Fostering Scholarly Communication

Research Article Open Access

Development and Validation of Nomogram for Predicting Upper Limb Lymphedema and Shoulder Joint Dysfunction Following Postoperative Radiotherapy in Breast Cancer

Chunming Lin[1#], Xuexiang Yan[2#], Xiang Feng[1#], Youjun Wu[1], Meizhen Shen[1], Xixi Wu[1], Feng Cen[1], Quanqing Zou[3*] and Jian Qin[1*]

[1]Department of Radiotherapy of the Clinical Oncology Center, The People's Hospital of Guangxi Zhuang Autonomous Region, Nanning, China

[2]Department of Radiation Therapy Physical Technology, The People's Hospital of Guangxi Zhuang Autonomous Region, Nanning, China

[3]Department of Breast Surgery, The People's Hospital of Guangxi Zhuang Autonomous Region, Nanning, China

#Co-first Authors

[*]**Corresponding Authors:** Jian Qin, Department of Radiotherapy III of the Clinical Oncology Center, The People's Hospital of Guangxi Zhuang Autonomous Region, Nanning, China, E-mail: janusy@126.com

Quanqing Zou, Department of Breast Surgery, The People's Hospital of Guangxi Zhuang Autonomous Region, Nanning, China, E-mail: zouquanqing@163.com

Received Date: July 07, 2025 **Accepted Date:** July 22, 2025 **Published Date:** July 25, 2025

Citation: Chunming Lin, Xuexiang Yan, Xiang Feng, Youjun Wu, Meizhen Shen, et al. (2025) Development and Validation of Nomogram for Predicting Upper Limb Lymphedema and Shoulder Joint Dysfunction Following Postoperative Radiotherapy in Breast Cancer. JJ Oncol Clin Res 6: 1-17

Abstract

Objective: Upper Limb Lymphedema (ULL) and Shoulder Joint Dysfunction (SJD) are common sequelae following breast cancer (BC) treatment, though their underlying pathophysiological mechanisms remain incompletely elucidated. This study aims to develop and validate a reliable nomogram for predicting the risk of ULL and SJD.

Methods: 122 BC patients who underwent surgery and radiotherapy from 2022 to 2024 were analyzed by univariate and multivariate logistic regression to identify factors affecting ULL and SJD, and to develop a nomogram. Nomograms were developed and evaluated using ROC curve, calibration curve, and decision curve analysis (DCA). Another 30 patients were used for validation of nomogram's accuracy and clinical utility.

Results: The univariate logistic regression indicated that axillary lymph node dissection (ALND), modified radical mastectomy (MRM), total number of lymph dissected nodes(TLN), AJCC 8th TNM stage, chest wall radiation (CW), internal mammary lymph drainage region radiation (IM_region), supra/infraclavicular region radiation (SI_region), minimum dose of axilla level I (I_Dmin), maximum dose of axilla level I (I_Dmax) , maximum dose of axilla levelIII (Ⅲ_Dmax), minimum dose of axillary cavity (ACDmin) were influencing factors of ULL ($P < 0.05$). Multivariate logistic regression analysis showed that I_Dmin, I_Dmax, ALND and MRM were independent risk factors for ULL ($P < 0.05$). A predictive nomogram incorporating these four variables was developed for ULL. Similarly, ALND, MRM, TLN, AJCC 8th TNM stage, CW, IM_region, SI_region, I_Dmin, I_Dmax, mean dose of axilla level I (I_Dmean), ACDmin were influencing factors of SJD ($P < 0.05$). Multivariate logistic regression analysis showed that I_Dmin, I_Dmax, ALND and MRM were independent risk factors for SJD ($P < 0.05$), based on which a SJD nomogram was built. ROC demonstrated that both ULL and SJD nomograms exhibited robust temporal stability and discriminative efficacy, with area under the curve (AUC) values of 0.891 and 0.910, respectively. The calibration curves exhibited satisfactory accuracy in both training and validation cohorts, showing excellent concordance between predicted probabilities and actual observations. DCA revealed superior clinical applicability of the nomograms.

Conclusions: The nomogram models—integrating radiation dose parameters (I_Dmin, I_Dmax), surgical factors (ALND, MRM), and externally validated—enable precise stratification of ULL and SJD risk. Clinically, this facilitates early intervention for high-risk patients and directly guides personalized radiation therapy planning, minimizing toxicity while preserving shoulder functionality and quality of life.

Keywords: Breast Cancer; Upper Limb Lymphedema; Shoulder Joint Dysfunction; Nomogram; Radiotherapy

Introduction

According to current epidemiological data, BC remains the most frequently diagnosed cancer among women globally and a leading cause of cancer-related mortality [1]. The therapeutic strategies for BC are multimodal, encompassing surgery, radiotherapy, chemotherapy, endocrine therapy, and targeted therapies [2, 3]. Surgery remains the cornerstone of BC management, while radiotherapy plays a pivotal role in preventing recurrence, with approximately 70% of patients requiring postoperative adjuvant radiotherapy [4, 5]. Rapid advancements in diagnostic and therapeutic technologies have contributed to a remarkable 91% 5-year survival rate for BC patients [6], resulting in a growing population of long-term survivor. The extended survival period has led to an increasing prominence of treatment-induced complications, whose detrimental effects on patients may outweigh those of the cancer itself. Among these complications, ULL and SJD are the most prevalent and severe, exerting profound impacts on patients' physical and psychological well-being as well as overall quality of life [7-11], however, their underlying pathogenic mechanisms remain poorly elucidated. Acute ULL is characterized by lymphatic fluid accumulation in the upper limbs, leading to swelling, heaviness, and paresthesia [12], whereas SJD manifests as restricted range of motion, pain, and function weakness [13]. Despite their high prevalence, the lack of reliable and comprehensive tools for predicting the risk of acute ULL and SJD has hindered the implementation of preventive measures or early interventions in clinical practice.

Current risk assessment for acute ULL and SJD primarily relies on clinicians' experience and limited factors such as age, AJCC 8th TNM stage, surgical approach, and radiation fields. However, these factors alone are insufficient to accurately predict the risk of these complications. Accumulating evidence indicates that both surgical procedures and radiotherapy are closely associated with the development of acute ULL and SJD. Notably, dosimetric parameters of radiotherapy, particularly the dose to the axillary region, may play a critical role in the pathogenesis of acute ULL and SJD [14]. Integrating these parameters into comprehensive predictive models could significantly enhance

risk stratification capabilities and provide a scientific foundation for developing individualized treatment strategies.

As a clinically widely adopted predictive tool, nomograms visually integrate key predictors to estimate individualized probabilities of disease occurrence. To date, few nomograms have been specifically developed and validated for predicting acute ULL and SJD in BC patients, highlighting the urgent need for such tools. In this study, we innovatively incorporated surgical and radiotherapy parameters to develop a nomogram predictive model for acute ULL and SJD, which demonstrated robust predictive performance in an independent validation cohort, thereby providing a reference framework for risk-stratified management of BC treatment-related complications.

Materials and Methods

Study Population

This single-center, retrospective cohort study consecutively enrolled breast cancer (BC) patients treated at the People's Hospital of Guangxi Zhuang Autonomous Region (GXPH). As illustrated in Figure 1, we employed a temporal split-cohort design:

Training cohort: 122 patients treated between June 2020 and December 2023

Validation cohort: 30 patients treated between June and August 2024

Patient identification occurred through systematic screening of the hospital's electronic medical records and radiotherapy registry using predefined inclusion/exclusion criteria. All participants underwent surgery followed by adjuvant radiotherapy at GXPH.

Inclusion Criteria

Patients were included if they met all of the following:

(a) Age 18-80 years;

(b) Histopathologically confirmed primary BC;

(c) Received MRM or breast-conserving surgery (BCS);

(d) Completed full course of adjuvant radiotherapy (≥90% planned dose);

(e) Documented Eastern Cooperative Oncology Group (ECOG) performance status 0-1;

(f) Expected survival >12 months;

(g) Voluntarily participated with intact cognitive and communication abilities;

(h) Had complete baseline and follow-up clinical records.

Exclusion Criteria

Patients were excluded if any of the following applied:

(a) Pre-existing ULL and/or shoulder joint disorders;

(b) Received <90% of planned radiation dose;

(c) Declined research participation;

(d) History of ipsilateral upper limb trauma or surgery;

(e) Male breast cancer;

(f) Recurrent disease, distant metastases, or concurrent malignancies;

(g) Unable to cooperate with the measurement;

(h) Incomplete arm circumference or Neer Shoulder Scoring System data.

Data Completeness Protocol

Missing data were addressed through:

Primary exclusion of cases with >20% missing core variables (per exclusion criterion h);

Targeted reconciliation for minor missing values (<5% of variables) via:

Re-examination of original clinical notes;

Verification against operative records;

Cross-referencing radiotherapy treatment logs;

Complete-case analysis after exhaustive reconciliation attempts. Participants were stratified into four complication subgroups: ULL-positive/negative and SJD-positive/negative. This study was approved by the Ethics Committee of GXPH (Approval No. KY-KJT-2023-97).

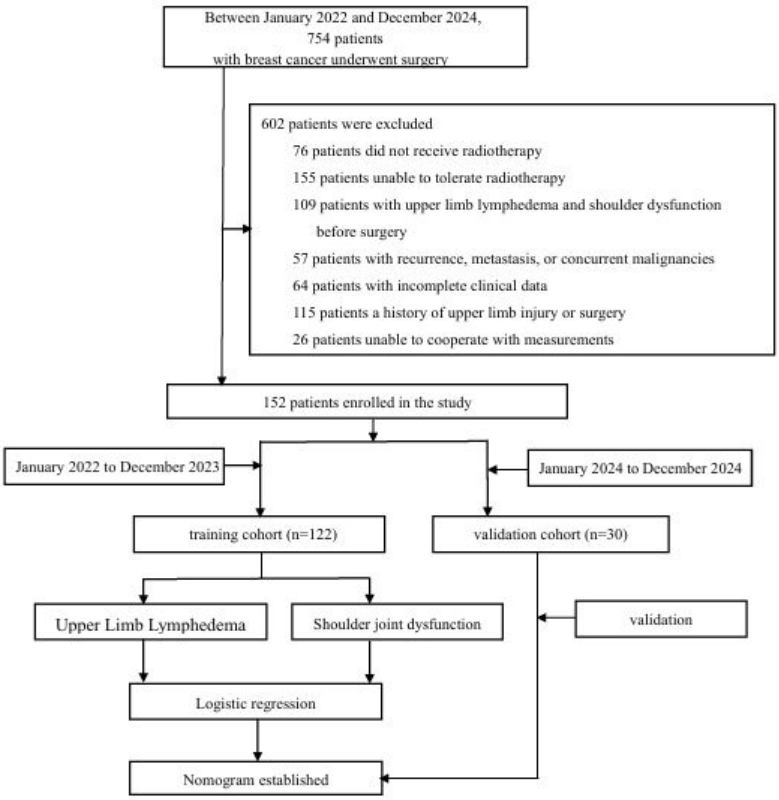

Figure 1: Flowchart

Data Collection

Clinical and pathological data were retrospectively collected from the study cohorts, including the following categories:

Demographic Characteristics

Age and menopausal status.

Surgical Parameters

a. Breast surgery type: BCS or MRM

b. Regional lymph node procedures: sentinel lymph node biopsy (SLNB) or ALND

Pathological Characteristics

a. TNM staging according to the 8th edition of the American Joint Committee on Cancer (AJCC) guidelines

b. TLN

c. Number of positive lymph nodes (PLN).

Radiotherapy

Radiotherapy protocol

Positioning: Supine position with both arms elevated, immobilized using an R612 carbon fiber fixation system (Clarity Medical, China) and M383 thermoplastic mask (ComeBetter, China) under free breathing. Surgical scars and breast contours were delineated with lead wire markers.

CT simulation: Contrast-enhanced scanning was performed using a Brilliance Big Bore CT simulator (Philips Healthcare, Netherlands) with intravenous ioversol injec-

tion (100 mL: 35 g, Hengrui Pharma, China). Scanning parameters: coverage from the mandible to the subdiaphragmatic region, slice thickness 4 mm.

Target volume delineation

Target volumes were delineated on CT simulation images using MIM Maestro software (v7.0.4; MIM Software Inc., USA) based on the ICRU Report 83 and the BC atlas published by the Radiation Therapy Oncology Group (RTOG). The irradiated regions were selected according to tumor stage, including:

Ipsilateral breast; chest wall (CW); internal mammary lymph drainage region (IM_region); supra/infraclavicular region (SI_region). Organs at risk (OARs) including axilla levels I-III, axillary cavity (AC), heart, and lungs were contoured following institutional protocols [15].

Prescription doses and OAR dose restriction

BCS: 50 Gy in 25 fractions of 2 Gy each, with sequential tumor bed boost of 10–16 Gy in 5–8 fractions (2 Gy/fraction)

MRM: 50 Gy in 25 fractions of 2 Gy each. OAR dose restriction for heart and lungs adhered to the Quantitative Analysis of Normal Tissue Effects in the Clinic (QUANTEC) recommendations. Dosimetric parameters of axillary regions (levels I-III and AC) were analyzed, including minimum dose (Dmin), maximum dose (Dmax), mean dose (Dmean), and dose-volume metrics (D/V). The associations between these parameters and acute ULL and SJD were evaluated.

Radiotherapy planning and delivery

Planning: Intensity-modulated radiation therapy (IMRT) [4, 5] plans were designed using Pinnacle treatment planning system (v9.10; Philips Healthcare, Netherlands) by board-certified medical physicists with over 10 years of BC radiotherapy experience.

Plan evaluation: All plans were reviewed and approved by radiation oncologists specializing in BC (≥10 years of experience, associate professor level or above).

Quality assurance: Dose verification was performed using an ArcCHECK® phantom (Sun Nuclear Corporation, USA) and a 3D water scanning system (BEAMSCAN®; PTW Freiburg, Germany).

Image-guided radiotherapy: Cone-beam CT (CBCT) with X-ray volume imaging system (v5.0.7.1) was utilized for daily setup correction (action thresholds: translational shifts <3 mm and rotational errors <1°).

Treatment delivery: IMRT [16] was administered via a Synergy® linear accelerator (Elekta, Sweden) using 6 MV X-rays ± electrons, with daily fractions (5 fractions/week).

ULL Assessment

Upper limb circumference differences between ipsilateral and contralateral arms were measured at 1 month post-radiotherapy to evaluate the impact of surgery and radiotherapy on acute ULL. Following the protocol described by Gencay et al. [17], standardized tape measurements (precision: 1 mm) were performed at five anatomical landmarks: the midpoint of the styloid process and 10 cm, 20 cm, 30 cm, and 40 cm proximal to the styloid process on both upper limbs. ULL was defined as a circumferential difference ≥2 cm between arms, consistent with the Chinese guidelines for the diagnosis and treatment of breast cancer-related lymphedema (2021 version).

SJD Assessment

Shoulder joint function was assessed preoperatively and 1 month post-radiotherapy using the Neer Shoulder Scoring System, which evaluates four domains: pain (35 points), functional ability (30 points), range of motion (25 points), and anatomical integrity (10 points), with a maximum total score of 100. Scores were categorized as excellent (>90), good (80-90), fair (70-79), or poor (≤70). SJD was defined as a decline in score category compared to baseline [12-13]. The effects of surgical and radiotherapeutic parameters on SJD development were analyzed.

Statistical Analysis

Statistical analyses were performed using R software (version 4.2.2; R Foundation for Statistical Computing, Austria).

Analytical Methods

Normally distributed continuous variables were expressed as$x\pm s$ and compared using independent samples t-test. Non-normally distributed variables were presented as median (interquartile range) and analyzed with *Mann-Whitney U* test. Categorical variables were described as frequencies (%) and compared via *Pearson's* chi-square or *Fisher's* exact test. A two-tailed $P<0.05$ was considered statistically significant.

Nomogram Development and Validation

Model construction: Variables with statistical significance in univariate analysis were incorporated into multivariable logistic regression models to construct nomograms for acute ULL and SJD.

Performance evaluation:

Discrimination: ROC curves with AUC;

Calibration: Calibration curves and Hosmer-Lemeshow test;

Clinical utility: DCA.

Validation: Model generalizability was assessed in the independent validation cohort.

Results

Group Comparisons

A total of 152 BC patients who underwent adjuvant radiotherapy with complete clinical records were included between June 2020 and August 2024, comprising a training cohort (n=122) and a validation cohort (n=30). The mean age was 48.3 ± 13.4 years (range: 25-73 years). In the derivation cohort, the incidence rates of acute upper limb lymphedema (ULL) and shoulder joint dysfunction (SJD) were 45.9% (56/122) and 47.5% (58/122), respectively. Corresponding rates in the validation cohort were 36.7% (11/30) and 43.3% (13/30).

Comparative analyses between complication-positive and complication-negative groups are summarized in Table 1. In the training cohort, significant differences ($P<0.05$) were observed between ULL/SJD-positive and negative groups for the following parameters: PLN, TLN, MRM, ALND, CW irradiation, SI_region irradiation, and dosimetric parameters including I_Dmin, I_Dmax, I_Dmean,III_Dmax, and ACDmin (Table 1). In the validation cohort, statistically significant variables ($P<0.05$) included TLN, ALND, SI_region irradiation, dosimetric parameters (dose, I_Dmin, Ⅱ_Dmin, Ⅱ_Dmean,III_Dmin,III_Dmean, ACDmin, ACDmean and Ⅱ_D/V) (Table 1).

Table 1: Comparison of clinical factors between the training cohort and validation cohort.

Variables	Total (n = 152)	Training cohort (n = 122)						Validation cohort (n = 30)					
		ULL			SJD			ULL			SJD		
		Absence (n = 66)	Presence (n = 56)	*P*	Absence (n = 64)	Presence (n = 58)	*P*	Absence (n = 19)	Presence (n = 11)	*P*	Absence (n = 17)	Presence (n = 13)	*P*
Stage, n (%)													
stage I	29 (19)	19 (29)	7 (12)	0.074	19 (30)	7 (12)	0.032	2 (11)	1 (9)	0.603	2(12)	1(8)	0.387
stage Ⅱ	72 (47)	28 (42)	26 (46)		28 (44)	26 (45)		12 (63)	6 (55)		11(65)	7(54)	
stageIII	51 (34)	19 (29)	23 (41)		17 (27)	25 (43)		5 (26)	4 (36)		4(23)	5(38)	
Surgery, n (%)													
Breast surgery													
BCS	80 (53)	47 (71)	13 (23)	< 0.001	47 (73)	13 (22)	< 0.001	15 (79)	5 (46)	0.108	12(71)	8(62)	0.608
MRM	72 (47)	19 (29)	43 (77)		17 (27)	45 (78)		4 (21)	6 (54)		5(29)	5(38)	
ALND													
0	53 (35)	39 (59)	6 (11)	< 0.001	39 (61)	6 (10)	< 0.001	5 (26)	3 (27)	0.955	7(41)	1(8)	0.043
1	99 (65)	27 (41)	50 (89)		25 (39)	52 (90)		14 (74)	8 (73)		10(59)	12(92)	

Pathology factor													
PLN, Median (Q1, Q3)	1 (0, 3)	0 (0, 2.75)	2 (0.75, 4)	0.002	0 (0, 1.25)	2 (1, 4)	< 0.001	0(1,3)	2(0,4)	0.793	1(0,3)	2(1.5,4)	0.251
TLN, Median (Q1, Q3)	15 (4.25, 22)	5 (3, 15)	17 (13, 21.25)	< 0.001	5 (3, 14.25)	17 (13.25, 21.75)	< 0.001	22(7,24)	27(14,31)	0.211	20(4,23.5)	25（22,30.5）	0.008
Radiation													
Radiation field													
CW, n (%)													
0	68 (45)	40 (61)	7 (12)	< 0.001	40 (62)	7 (12)	< 0.001	15 (79)	6 (55)	0.167	12(71)	9(69)	0.937
1	84 (55)	26 (39)	49 (88)		24 (38)	51 (88)		4 (21)	5 (45)		5(29)	4(31)	
SI_region, n (%)													
0	61 (40)	40 (61)	14 (25)	< 0.001	40 (62)	14 (24)	< 0.001	5 (26)	2 (18)	0.618	7(41)	0(0)	0.009
1	91 (60)	26 (39)	42 (75)		24 (38)	44 (76)		14 (74)	9 (82)		10(59)	13(100)	
IM_region, n (%)													
0	103(68)	53 (80)	36 (64)	0.075	52 (81)	37 (64)	0.05	10 (53)	4 (36)	0.397	10(59)	4(31)	0.133
1	49 (32)	13 (20)	20 (36)		12 (19)	21 (36)		9 (47)	7 (64)		7(41)	9(69)	
Dosimetry factor													
Dose, Median (Q1, Q3)	58.40 (50.00, 58.40)	58.40 (50.00, 59.12)	53.50 (50.00, 59.36)	0.624	58.40 (50.00, 59.36)	51.75 (50.00, 59.36)	0.42	58.4 (58.40, 58.40)	58.4 （50.00, 58.40）	0.605	58.4 (58.40, 58.40)	58.4 （50.00, 58.40）	0.037
I_Dmin, □x±s	2568.92 ± 1477.17	1932.52 ± 977.59	2804.24 ± 1300.24	< 0.001	1893.8 ± 965.29	2816.91 ± 1280.74	< 0.001	3195.37 ± 2103.64	4107.25 ± 1772.29	0.033	2512.28 ± 2172.36	4860.23 ± 248.41	0.001
I_Dmax, Median (Q1, Q3)	5326.90 (5047.08, 5634.9)	5170 (5034.32, 5442.4)	5467.25 (5109.6, 5902.52)	0.008	5168.5 (5033.42, 5433.4)	5461.75 (5113.1, 5889.22)	0.006	5402.60 (5010.40,5454.80)	5394.50 (5294.40,5405.80)	0.813	5338.50 (4851.10,5471.60)	5405.40 (5363.35,5434.25)	0.25
I_Dmean, Median (Q1, Q3)	4282.05 (3480.35, 4946.5)	3983.95 (3453.52, 4391.1)	4386.45 (3520.85, 4870.18)	0.04	3976.95 (3444.7, 4376.4)	4424.7 (3549.6, 4876.52)	0.017	5174.40 (1551.40,5233.20)	5181.20 (5135.90,5252.80)	0.237	5134.70 (1369.95,5233.45)	5191.40 (5174.70,5248.00)	0.063
I_D/V, Median (Q1,Q3)	152.95 (74.80, 259.37)	102.55 (72.3, 230.03)	143.55 (71.85, 233.25)	0.6	102.55 (71.6, 225.47)	143.55 (75.62, 237.65)	0.535	237.22 (136.94,261.81)	263.69 (162.58,418.36)	0.272	223.58 (95.54,307.59)	241.15 (203.75,278.21)	0.305
Ⅱ_Dmin, Median (Q1, Q3)	3162.05 (1056.25, 4240.1)	2924.2 (1056.25, 3797.1)	2911.75 (900.7, 4239.92)	0.646	2887.2 (1038.6, 3723.73)	3106.1 (998.77, 4190.25)	0.45	3723.60 (602.70,4286.50)	4281.30 (2264.30,4755.60)	0.175	3172.30 (418.70,4019.00)	4286.50 (3842.90,4462.10)	0.016
Ⅱ_Dmax, Median (Q1, Q3)	5244.20 (4671.25, 5506.3)	5051.8 (4630.42, 5441.0)	5316.3 (4264.65, 5746.5)	0.311	5038.85 (4619.1, 5419.48)	5371.8 (4310.5, 5736.32)	0.205	5341.90 (5258.50,5486.30)	5378.90 (5304.90,5433.10)	0.763	5341.90 (5142.25,5484.90)	5378.90 (5323.25,5426.35)	0.403
Ⅱ_Dmean, Median (Q1, Q3)	4462.10 (3048.95, 5098.7)	4083.55 (2724.55, 5067.1)	4424.95 (3021.45, 5135.15)	0.343	4025.35 (2676.43, 5049.5)	4450.95 (3099.6, 5137.12)	0.225	4883.90 (3187.60,5100.60)	5052.70 (4901.10,5180.40)	0.107	4677.20 (2741.10,5023.75)	5093.10 (5014.70,5135.90)	0.009
Ⅱ_D/V, Median (Q1,Q3)	261.15 (150.30, 417.70)	262.2 (144.27, 401.9)	323.25 (186.02, 469.45)	0.169	262.2 (141.98, 416.05)	309.85 (185.68, 466.57)	0.214	186.55 (127.36,242.62)	239.94 (132.92,319.13)	0.401	157.29 (123.41,218.56)	243.38 (167.06,287.09)	0.025
Ⅲ_Dmin, Median (Q1, Q3)	2717.35 (1325.55, 3977.0)	2800.7 (1283.2, 4156.8)	2908.7 (1320, 4145.82)	0.742	2793.75 (1245.7, 4090.28)	3034.75 (1422.0, 4224.48)	0.453	2197.60 (1322.40,2709.90)	2864.00 (1935.30,4004.50)	0.061	(1369.95,5233.45)	3042.70 (2350.15,3265.10)	0.009
Ⅲ_Dmax, Median (Q1, Q3)	4769.85 (3227.15, 5389.7)	4823.1 (3612.62, 5467.6)	3751.55 (2280.33, 5189.9)	0.03	4769.85 (3489.3, 5422.52)	3935.55 (2310.1, 5248.02)	0.1	5113.00 (4807.10,5387.20)	5179.90 (4907.90,5390.60)	0.78	1883.90 (594.05,2509.00)	5213.60 (5067.90,5339.95)	0.325
Ⅲ_Dmean, Median (Q1, Q3)	3915.60 (2222.58, 5041.4)	4091.95 (1812.28, 5171.9)	3373.65 (2217.4, 5018.25)	0.581	3600.9 (1736.5, 5169.35)	3539.5 (2260.0, 5039.85)	0.92	4054.60 (3711.80,4257.40)	4183.20 (3975.50,4705.50)	0.312	5030.30 (4702.50,5391.40)	4225.80 (4059.05,4515.10)	0.047

Ⅲ_D/V, Median (Q1,Q3)	213.40 (119.91, 378.10)	241 (102.38, 376.8)	231.7 (107.05, 444.7)	0.706	241 (95.17, 388.5)	231.7 (110.55, 442.72)	0.714	188.15 (129.44,211.59)	190.49 (123.35,359.89)	0.451	137.09 (121.52,228.35)	199.42 (179.76,345.11)	0.069
ACDmin, Median (Q1, Q3)	3364.00 (2304.33, 4474.2)	3384.4 (2342.73, 4487.1)	4160.65 (3175.52, 4662.98)	0.02	3364 (2319.85, 4469.3)	4160.65 (3221.6, 4667.32)	0.01	1867.40 (326.80,2433.90)	2664.40 (752.80,3789.50)	0.061	3975.50 (2918.50,4237.80)	2664.40 (2084.60,3048.60)	0.008
ACDmax, x̄±s	5441.94 ± 328.74	5406.03 ± 302.4	5502.45 ± 405.17	0.145	5400.82 ± 305.59	5504.88 ± 398.28	0.111	5407.92 ± 163.97	5408.06 ± 231.78	0.88	5384.74 ± 247.84	5438.35 ± 37.91	0.49
ACDmean, Median (Q1,Q3)	4806.05 (4087.70, 5084.4)	4857 (4039.2, 5121.4)	4818.7 (4168.7, 5096.33)	0.961	4824.75 (4012.6, 5110.95)	4837.9 (4205.9, 5097.38)	0.703	4676.30 (2930.40,4878.80)	4816.50 (4700.00,4993.30)	0.149	4463.90 (2307.70,4815.70)	4848.20 (4743.95,4957.90)	0.016
ACD/V, Median (Q1,Q3)	356.35 (58.96, 914.28)	563.75 (263.17, 940.08)	459.8 (97.5, 1005.02)	0.522	527.3 (240.82, 935.22)	486.5 (104.58, 1001.78)	0.684	48.94 (32.18,59.1)	48.82 (30.86,92.07)	0.533	39.65 (28.94,59.38)	53.33 (42.69,74.84	0.09

Stage: tumor stage; PLN: number of positive lymph nodes; TLN: total number of dissected lymph nodes; Dose: prescription dose that patients received; I_Dmin: minimum dose of axilla level I; I_Dmax: maximum dose of axilla level I; I_Dmean: mean dose of axilla level I; I_D/V: mean dose/volume of axilla level I; Ⅱ_Dmin: minimum dose of axilla level Ⅱ; Ⅱ_Dmax: maximum dose of axilla level Ⅱ; Ⅱ_Dmean: mean dose/volume of axilla level Ⅱ; Ⅱ_D/V: mean dose/volume of axilla level Ⅱ; III_Dmin: minimum dose of axilla level III; III_Dmax: maximum dose of axilla level III; III_Dmean: mean dose of axilla level III; III_D/V: mean dose/volume of axilla level III; ACDmin: minimum dose of axillary cavity; ACDmax: maximum dose of axillary cavity; ACDmean: mean dose of axillary cavity; ACD/V: mean dose/volume of axillary cavity.

Nomogram Development and Validation

ULL Nomogram Development and Validation

Univariate logistic regression analysis identified ALND, MRM, AJCC 8th TNM stage, CW irradiation, IM_region irradiation, SI_region irradiation, I_Dmin, I_Dmax, II-I_Dmax and ACDmin as significant factors of acute ULL (all $P< 0.05$; Table 2). Multivariable analysis revealed four independent risk factors for acute ULL following BC treatment: I_Dmin (OR = 2.20, 95% CI: 1.11–4.38; $P = 0.026$), I_Dmax (OR = 1.12, 95% CI: 1.05–1.20; $P < 0.001$), ALND (OR = 151.44, 95% CI: 4.22–4544; $P < 0.001$), and MRM (OR = 67.91, 95% CI: 2.44–1892.49; $P = 0.013$) (Table 2).

A nomogram incorporating these four predictors was developed to estimate individualized ULL risk (Figure 2). Calibration curves demonstrated excellent agreement between predicted and observed results in both cohorts, with close alignment to the ideal reference line (Figure 3A-B). The Hosmer-Lemeshow test confirmed good model fit ($P = 0.378$), indicating no significant deviation between predicted and actual outcomes. ROC analysis yielded AUC values of 0.891 (training cohort) and 0.828 (validation cohort) (Figure 3C-D), indicating robust discriminative ability and model stability. DCA demonstrated favorable clinical utility across a wide threshold probability range in both cohorts, with net benefit gains over default strategies (Figure 3E-F).

SJD Nomogram Development and Validation

Univariate logistic regression identified ALND, MRM, TLN, AJCC 8th TNM stage, CW irradiation, IM_region irradiation, SI_region irradiation, I_Dmin, I_Dmax, I_Dmean and ACDmin as significant factors of SJD (all $P < 0.05$; Table 3). Multivariable analysis demonstrated four independent risk factors for SJD: I_Dmin (OR = 1.13, 95% CI: 1.07–1.20; $P < 0.001$), I_Dmax (OR = 2.61, 95% CI: 1.46–4.68; $P = 0.001$), ALND (OR = 181.53, 95% CI: 5.79–287.52; $P = 0.003$) and MRM (OR = 19.88, 95% CI: 1.49–265.28; $P = 0.024$) (Table 3).

A nomogram incorporating these four variables was established to stratify SJD risk (Figure 4). Calibration curves demonstrated excellent agreement between predicted probabilities and observed outcomes in both cohorts (Figure 5A-B). The Hosmer-Lemeshow test confirmed good model fit ($P = 0.247$), indicating no significant miscalibration. ROC analysis revealed high discriminative performance with AUC values of 0.910 (training cohort) and 0.864 (validation cohort) (Figure 5C-D), demonstrating both stability and generalizability. DCA demonstrated superior net benefit gains for SJD prediction compared to "treat-all" or "treat-none" strategies across both cohorts (Figure

5E-F).

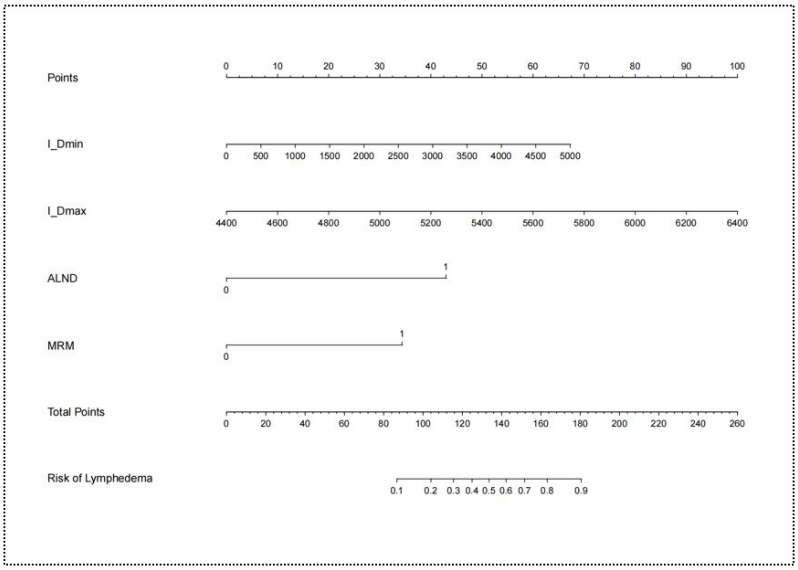

Figure 2: Nomogram of ULL

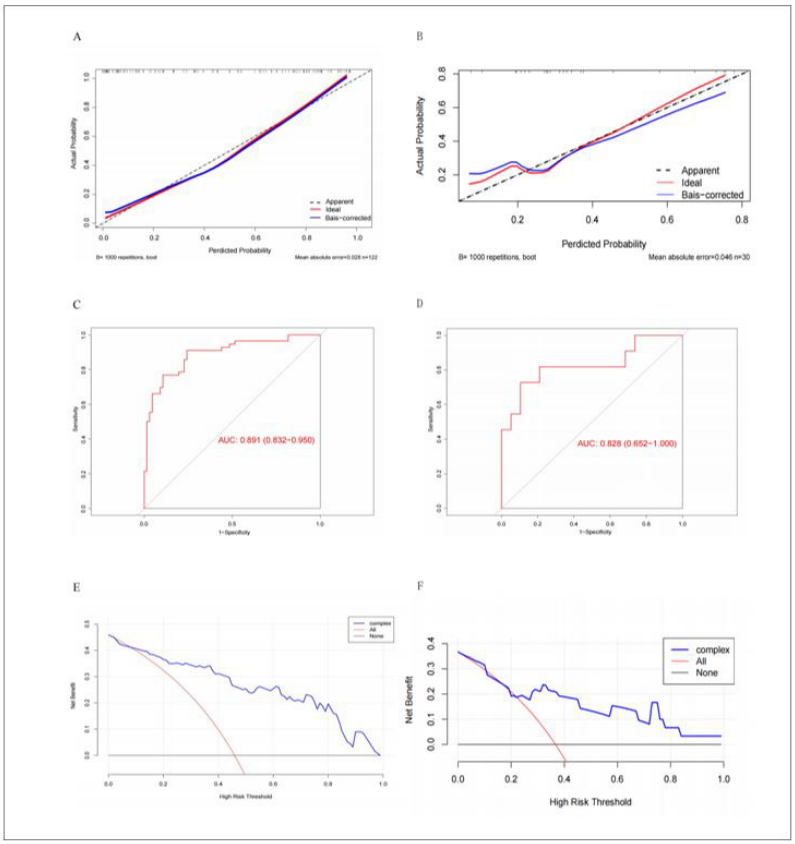

Figure 3: Calibration curves of (A) training set and (B) validation set in the ULL normogram. ROC curves and the area under the curve of (C) Training set and (D) validation set in the ULL normogram. DCA curves of (E) the training set and (F) the validation set in the ULL normogram.

Table 2: The univariate and multivariate logistic regression of ULL

Characteristics	Univariate analysis			Multivariate analysis		
	OR	CI	*P*	OR	CI	*P*
Stage	3.29	1.14-9.47	0.028	1.79	0.08-41.46	0.716
ALND	12.04	4.52-32.03	<0.001	151.44	4.22-4544	<0.001
MRM	8.18	3.61-18.54	<0.001	67.91	2.44-1892.49	0.013
PLN	1.03	0.96-1.1	0.441	NA	NA	NA
TLN	1.11	1.06-1.16	<0.001	1.05	0.95-1.17	0.344
CW	10.77	4.24-27.38	<0.001	5.32	0.27-106.51	0.275
IM_region	2.26	1-5.12	0.05	NA	NA	NA
SI_region	4.62	2.11-10.08	<0.001	0.05	0-1.14	0.06
Dose	0.96	0.89-1.03	0.273	NA	NA	NA
I_Dmin	1	0.98-0.99	<0.001	2.20	1.11-4.38	0.026
I_Dmax	1	0.98-0.99	0.005	1.12	1.05-1.20	<0.001
I_Dmean	1	0.99-1.01	0.055	NA	NA	NA
I_D/V	1	0.93-1.02	0.622	NA	NA	NA
II_Dmin	1	0.66-2.62	0.666	NA	NA	NA
II_Dmax	1	0.82-5.6	0.721	NA	NA	NA
II_Dmean	1	0.43-2.81	0.335	NA	NA	NA
II_D/V	1	0.98-1.02	0.157	NA	NA	NA
III_Dmin	1	0.55-5.2	0.801	NA	NA	NA
III_Dmax	1	0.98-0.99	0.024	NA	NA	NA
III_Dmean	1	0.71-4.36	0.665	NA	NA	NA
III_D/V	1	0.68-3.23	0.682	NA	NA	NA
ACDmin	1	0.97-0.99	0.035	NA	NA	NA
ACDmax	1	0.99-1.02	0.136	NA	NA	NA
ACDmean	1	0.93-1.06	0.758	NA	NA	NA
ACD/V	1	0.92-1.03	0.568	NA	NA	NA

Table 3: The univariate and multivariate logistic regression of SJD

Characteristics	Univariate analysis			Multivariate analysis		
	OR	CI	*P*	OR	CI	*P*
Stage	3.99	1.38-11.56	0.011	0.25	0.01-4.11	0.33
ALND	13.52	5.06-36.13	<0.001	181.53	5.79-287.52	0.003
MRM	9.57	4.17-21.94	<0.001	19.88	1.49-265.28	0.024
PLN	1.08	0.99-1.16	0.07	NA	NA	NA

TLN	1.12	1.07-1.18	<0.001	1.06	0.95-1.19	0.307
CW	12.14	4.75-31.03	<0.001	2.65	0.17-41.79	0.489
IM_region	2.46	1.08-5.61	0.033	5.38	0.8-36	0.083
SI_region	5.24	2.39-11.5	<0.001	0.28	0.04-2.24	0.231
Dose	0.95	0.88-1.02	0.153	NA	NA	NA
I_Dmin	1	0.98-0.99	<0.001	1.13	1.07-1.20	<0.001
I_Dmax	1	0.98-0.99	0.005	2.61	1.46-4.68	0.001
I_Dmean	1	0.96-0.98	0.025	NA	NA	NA
I_D/V	1	0.43-2.32	0.595	NA	NA	NA
II_Dmin	1	0.72-3.86	0.469	NA	NA	NA
II_Dmax	1	0.76-4.13	0.544	NA	NA	NA
II_Dmean	1	0.83-2.69	0.212	NA	NA	NA
II_D/V	1	0.42-2.2	0.206	NA	NA	NA
III_Dmin	1	0.51-2.95	0.516	NA	NA	NA
III_Dmax	1	0.89-1.71	0.059	NA	NA	NA
III_Dmean	1	0.82-6.23	0.972	NA	NA	NA
III_D/V	1	0.62-5.36	0.735	NA	NA	NA
ACDmin	1	0.88-0.93	0.019	NA	NA	NA
ACDmax	1	0.61-8.64	0.108	NA	NA	NA
ACDmean	1	0.83-6.82	0.547	NA	NA	NA
ACD/V	1	0.53-10.12	0.735	NA	NA	NA

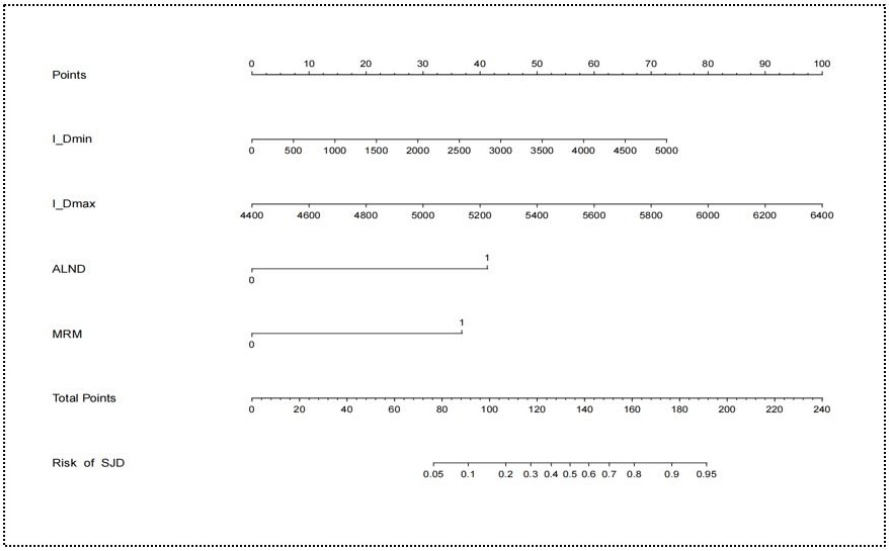

Figure 4: Nomogram of SJD

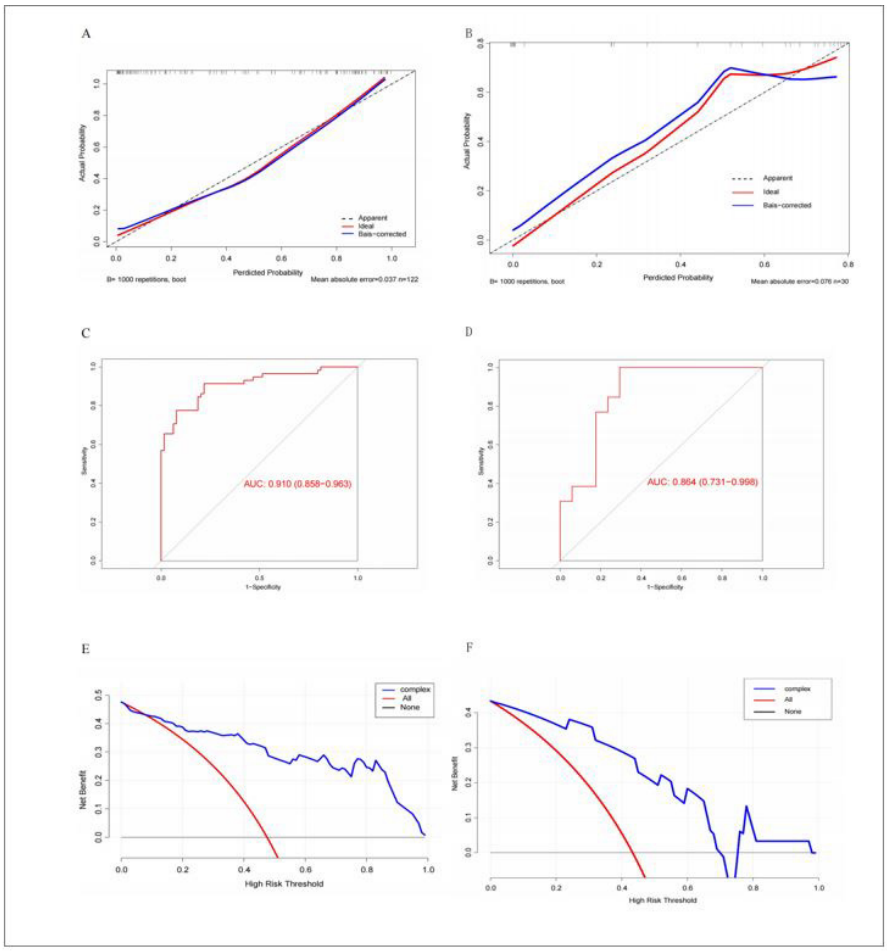

Figure 5: Calibration curves of (A) training set and (B) validation set in the ULL normogram. ROC curves and the area under the curve of (C) Training set and (D) validation set in the ULL normogram. DCA curves of (E) the training set and (F) the validation set in the ULL normogram.

Discussion

This study developed and validated dual nomograms integrating surgical (ALND, MRM) and dosimetric (I_Dmin, I_Dmax) predictors for ULL and SJD in BC patients. Crucially, we identified that both complications share identical risk factors—surgical extent (ALND/MRM) and axillary dose distribution (I_Dmin, I_Dmax)—enabling their consolidation into a single unified predictive framework. This integration streamlines clinical workflows, allowing simultaneous ULL/SJD risk quantification during treatment planning. Our findings confirm established surgical mechanisms: ALND/MRM drive lymphatic disruption and biomechanical impairment [14, 18-22], while extending Gross et al.'s [23] anatomical observations by quantifying dose-dependent relationships at axillary level I. Specifically, elevated I_Dmin/I_Dmax significantly increased ULL/SJD risk —transforming qualitative associations into actionable dosimetric thresholds. The model's integration of surgery and radiotherapy parameters reflects the synergistic pathophysiology of these complications: surgical dissection primes the axilla for radiation-induced fibrosis, while dose hotspots (I_Dmax) exacerbate tissue stiffening and fluid stagnation. By capturing this synergy through shared predictors, our nomogram offers clinicians a practical "one-stop" risk assessment tool, enhancing efficiency in busy oncology settings where rapid decision-making is critical.

Mechanistically, these parameters emerged as significant predictors because axillary level I basin constitutes a critical anatomic nexus for both lymphatic drainage and shoulder biomechanics. Breast surgery and axilla exploration routinely involve level I axillary lymph node basin dissection [24], adversely affecting shoulder function. Surgical dissection via ALND or MRM induces a triple insult: (1) - lymphovenous disconnection, (2) neurovascular microtrau-

ma, and (3) fascial destabilization. These create a permissive environment for radiation damage by compromising intrinsic tissue repair capacity. Radiotherapy has also been implicated in ULL/SJD pathogenesis [25]; postoperative radiation can induce tissue edema, muscle contracture, and fibrosis, critically compromising fluid transport and mobility in the affected limb [26]. Since the axilla level I is not a conventional radiation field, dose constraints for this lymphatic drainage region ise crucial for ULL and shoulder function.

Currently, our risk prediction model comprises a nomogram, equation, and risk table. Like most existing models, ours employs a nomogram. Published models report moderate-to-excellent predictive performance (AUC: 0.680–0.908) [27-31], influenced by variations in study populations, candidate predictors, and modeling methods. Most incorporate readily measurable predictors, enhancing clinical applicability and patient self-management utility.

Previous studies established foundational relationships between surgery/radiotherapy and ULL/SJD, they exhibited critical limitations: (1) oversimplification of radiotherapy parameters (e.g., dose, radiation exposure (yes/no) and similar radiation fields), (2) fragmented pathophysiological frameworks treating ULL and SJD as isolated endpoints, and (3) Lack of discussion on the dosimetry important lymphatic drainage areas (e.g., Gross, Liu, and Yuan et al.) [32-34]. Few have explored dose effects within regional lymphatic drainage areas. Our findings identify I_Dmin and I_Dmax as significant ULL/SJD predictors, suggesting dose constraints to lymphatic regions may mitigate risk. The nomogram demonstrated high accuracy (AUC: 0.891 for ULL, 0.910 for SJD), enabling personalized risk stratification and early rehabilitation targeting, with decision curve analysis confirming clinical net benefit. Based on the risk probability derived from this model, a prophylaxis-driven decision tree was constructed: low-risk patients (<15% probability) receive standard care; intermediate-risk (15-35%) trigger intensified rehabilitation; high-risk (>35%) initiates active rehabilitation therapy with personalized dosimetric constraints.

While this study establishes the prognostic value of integrated surgical-dosimetric modeling, several limitations warrant consideration. The single-center, retrospective design inherently restricts participant diversity, with our cohort drawn from a geographically homogeneous population (85% Han Chinese) treated under uniform institutional protocols. This limits generalizability to healthcare systems employing alternative rehabilitation pathways or populations with divergent body composition profiles. Concurrently, the modest sample size (n=122) constrains analytical granularity in three critical dimensions: (1) precluding meaningful evaluation of interaction effects between surgical approach (ALND vs. MRM) and radiation dose gradients, (2) impeding risk stratification across BMI extremes (<18.5 or >35 kg/m^2) where adipose tissue may modulate fibrosis susceptibility, and (3) restricting assessment of reconstruction-specific morbidity patterns (implant-based vs. autologous). Moreover, the relatively small size of the validation cohort (n=30) may potentially introduce bias into the results. Critically, the absence of external validation represents a fundamental constraint on clinical implementation. Our high discriminative performance (AUC >0.89) may reflect institution-specific treatment practices rather than inherent model robustness. This uncertainty is compounded by unmeasured confounders with established pathophysiological relevance: variations in postoperative rehabilitation adherence (directly influencing muscle pump efficacy), aerobic exercise frequency (modulating inflammatory cytokine profiles), and undetailed DVH parameters beyond I_Dmin/I_Dmax (e.g., V20 of brachial plexus). These omissions may partially explain residual outcome variance despite model optimization.

To advance this nomogram from predictive tool to clinical adaptive applicability tool, we propose: (1) Dynamic biomarker integration through prospective serum proteomic profiling (IL-6, VEGF-C, TGF-β1 at baseline; MMP-9/TIMP-1 at post-RT week 4; sICAM-1/HA at month 3), enabling machine learning-enhanced risk stratification via longitudinal cytokine tracking; (2) Closed-loop AI optimization through DICOM-RT integrated neural networks that auto-contour level I basins (DSC >0.90), compute real-time I_Dmin/I_Dmax, and dynamically adjust dose constraints during plan optimization using AI algorithms; and (3) Precision prevention frameworks combining biomarker-refined risk scores with automated treatment plan modulation, clinically implemented via API-driven TPS plugins (Eclipse/MOSAIQ). This pipeline—currently in prototype testing—-

would translate static predictions into adaptive interventions, where biomarker trends trigger preemptive rehabilitation referrals while AI-driven dosimetric avoidance reduces biomechanical strain. This holds significant importance for both social and economic aspects.

This validated tool provides clinically actionable simultaneous risk estimation, facilitating: (1) personalized rehabilitation triage where low-risk patients (<15% probability) receive standard surveillance, while high-risk cases (>35%) initiate early pneumatic compression/physical therapy; and (2) radiation dose optimization through real-time I_Dmin/I_Dmax constraint guidance during treatment planning. To maximize translational impact, future research should prioritize multicenter validation across home and abroad populations to establish region-specific calibration coefficients, DICOM-RT API integration with auto--contouring of level I basins for instantaneous risk display in clinical systems (Eclipse/MOSAIQ), and prospective incorporation of fibrosis biomarkers (TGF-β1, HA) to develop adaptive risk models that dynamically update during treatment. This three-phase roadmap—validation, technical implementation, and biomarker refinement—will transform the nomogram from static predictor to adaptive prevention catalyst, ultimately enabling automated dose-painting strategies that selectively spare lymphatic corridors.

Conflict of interest

The authors have no conflicts of interest to declare.

Funding

Guangxi Science and Technology Base and Talent Special Project (Number: Gui Ke AD23026097)

References

1. Kim J, Harper A, et al. (2025) Global patterns and trends in breast cancer incidence and mortality across 185 countries. Nat Med.

2. de Boniface J, Filtenborg Tvedskov T, et al. (2024) Omitting Axillary Dissection in Breast Cancer with Sentinel-Node Metastases. N Engl J Med. 390:1163-75.

3. Kuemmel S, Harper-Wynne C, et al. (2024) heredERA Breast Cancer: a phase III, randomized, open-label study evaluating the efficacy and safety of giredestrant plus the fixed--dose combination of pertuzumab and trastuzumab for subcutaneous injection in patients with previously untreated HER2-positive, estrogen receptor-positive locally advanced or metastatic breast cancer. BMC Cancer. 24: 641.

4. Kunkler IH, Williams LJ, et al. (2023) Breast-Conserving Surgery with or without Irradiation in Early Breast Cancer. N Engl J Med. 388: 585-94.

5. Williams LJ, Kunkler IH, et al. (2024) Postoperative radiotherapy in women with early operable breast cancer (Scottish Breast Conservation Trial): 30-year update of a randomised, controlled, phase 3 trial. Lancet Oncol. 25: 1213-21.

6. Siegel RL, Giaquinto AN, Jemal A (2024) Cancer statistics, 2024. CA Cancer J Clin. 74: 12-49.

7. Koelmeyer LA, Gaitatzis K, et al. (2022) Risk factors for breast cancer-related lymphedema in patients undergoing 3 years of prospective surveillance with intervention. Cancer. 128: 3408-15.

8. Shah C, Boyages J, Kang, et al. (2024) Timing of Breast Cancer Related Lymphedema Development Over 3 Years: Observations from a Large, Prospective Randomized Screening Trial Comparing Bioimpedance Spectroscopy (BIS) Versus Tape Measure. Ann Surg Oncol. 31: 7487-95.

9. Huo M, Zhang X, et al. (2024) Short-term effects of a new resistance exercise approach on physical function during chemotherapy after radical breast cancer surgery: a randomized controlled trial. BMC Womens Health. 24: 160.

10. Pondeenana S, Saenghirunvattana C, et al. (2023) Additional intraoperative subpectoral plane block vs conventional pain control: A comparison of shoulder movement in patients with mastectomy. Breast. 72: 103579.

11. Guloglu S, Basim P, Algun ZC (2023) Efficacy of proprioceptive neuromuscular facilitation in improving shoulder biomechanical parameters, functionality, and pain after axillary lymph node dissection for breast cancer: A randomized controlled study. Complement Ther Clin Pract.50: 101692.

12. Duygu-Yildiz E, Bakar Y, Hizal M (2023) The effect of complex decongestive physiotherapy applied with different compression pressures on skin and subcutaneous tissue thickness in individuals with breast cancer-related lymphedema: a double-blinded randomized comparison trial. Support Care Cancer. 31: 383.

13. Leung AKP, Ouyang H, Pang MYC (2023) Effects of mechanical stimulation on mastectomy scars within 2 months of surgery: A single-center, single-blinded, randomized controlled trial. Ann Phys Rehabil Med. 66: 101724.

14. Whelan TJ, Olivotto IA, et al. (2015) Regional Nodal Irradiation in Early-Stage Breast Cancer. N Engl J Med. 373: 307-16.

15. White J, Tai A, Arthur DA, et al. Breast cancer atlas for radiation therapy planning: Consensus.

16. Choi KH, Ahn SJ, et al. (2021) Postoperative radiotherapy with intensity-modulated radiation therapy versus 3-dimensional conformal radiotherapy in early breast cancer: A randomized clinical trial of KROG 15-03. Radiother Oncol. 154: 179-86.

17. Gencay Can A, Can SS, et al. (2018) Is kinesiophobia associated with lymphedema, upper extremity function, and psychological morbidity in breast cancer survivors? Turk J Phys Med Rehabil. 65: 139-46.

18. Bartels SAL, Donker M, et al. (2023) Radiotherapy or Surgery of the Axilla After a Positive Sentinel Node in Breast Cancer: 10-Year Results of the Randomized Controlled EORTC 10981-22023 AMAROS Trial. J Clin Oncol. 41: 2159-65.

19. Rockson, SG, Keeley, V, et al. (2019) Cancer-associated secondary lymphoedema. Nat. Rev. Dis. Prim. 5: 22.

20. Bartels SAL, Donker M, et al. (2023) Radiotherapy or Surgery of the Axilla After a Positive Sentinel Node in Breast Cancer: 10-Year Results of the Randomized Controlled EORTC 10981-22023 AMAROS Trial. J Clin Oncol. 41: 2159-65.

21. Woo, KJ, Lee, KT, et al. (2018) Effect of breast reconstruction modality on the development of postmastectomy shoulder morbidity. J. Plast. Reconstr. Aesthet. Surg. 71: 1761–7.

22. Penn, I-W, Chang, Y-C, et al. (2019) Risk factors and prediction model for persistent breast-cancer-related lymphedema: A 5-year cohort study. Support. Care Cancer. 27: 991–1000.

23. Gross, JP, Sachdev, S, et al. (2018) Radiation Therapy Field Design and Lymphedema Risk After Regional Nodal Irradiation for Breast Cancer. Int. J. Radiat. Oncol. Biol. Phys. 102: 71–8.

24. Almahariq MF, Maywood MJ, et al. (2020) Mapping of Metastatic Level I Axillary Lymph Nodes in Patients with Newly Diagnosed Breast Cancer. Int J Radiat Oncol Biol Phys. 106: 811-20.

25. Reimer T, Stachs A, et al. (2025) Axillary Surgery in Breast Cancer - Primary Results of the INSEMA Trial. N Engl J Med. 392: 1051-64.

26. Gross, JP, Lynch, et al. (2019) Determining the Organ at Risk for Lymphedema After Regional Nodal Irradiation in Breast Cancer. Int. J. Radiat. Oncol. Biol. Phys. 105: 649–58.

27. Lin Q, Yang T, et al. (2022) Prediction models for breast cancer-related lymphedema: a systematic review and critical appraisal. Syst Rev. 11: 217.1; 116: 1218-25.

28. Kim JS, Kim JH, et al. (2022) Prediction of breast cancer-related lymphedema risk after postoperative radiotherapy via multivariable logistic regression analysis. Front Oncol. 12: 1026043.

29. Park YI, Chang JS, et al. (2023) Development and Validation of a Normal Tissue Complication Probability Model for Lymphedema After Radiation Therapy in Breast Cancer. Int J Radiat Oncol Biol Phys. 116: 1218-25.

30. Chou YH, Liao SF, et al. (2025) The incidence of and risk factors for axillary web syndrome with limited shoulder movement after surgery for breast cancer, and the effect of early physical therapy intervention. Discov Oncol. 16: 7.

31. Levy EW, Pfalzer LA, et al. (2012) Predictors of functional shoulder recovery at 1 and 12 months after breast cancer surgery. Breast Cancer Res Treat. 134: 315-24.

32. Gross JP, Whelan TJ, et al. (2019) Development and Validation of a Nomogram to Predict Lymphedema After Axillary Surgery and Radiation Therapy in Women With Breast Cancer From the NCIC CTG MA.20 Randomized Trial. Int J Radiat Oncol Biol Phys. 105: 165-73.

33. Liu YF, Liu JE, et al. (2021) Development and validation of a nomogram to predict the risk of breast cancer-related lymphedema among Chinese breast cancer survivors. Support Care Cancer. 29: 5435-45.

34. Yuan Q, Hou J, et al. (2021) Development and Validation of an Intraoperative Nomogram to Predict Breast Cancer-Related Lymphedema Based on the Arm Lymphatics Distribution. Ann Surg Oncol. 28: 7319-28.